

Pseudogap in the microwave response of $\text{YBa}_2\text{Cu}_3\text{O}_{7-x}$

M.R. Trunin, Yu.A. Nefyodov, and A.F. Shevchun

Institute of Solid State Physics RAS, 142432 Chernogolovka, Moscow district, Russia

The in-plane and out-of-plane surface impedance and microwave conductivity components of one and the same $\text{YBa}_2\text{Cu}_3\text{O}_{7-x}$ ($0.07 \leq x \leq 0.47$) single crystal are determined in the wide ranges of temperature T and carrier concentration p in CuO_2 planes. The following features of the superfluid density $n_s(T, p) \propto \lambda_{ab}^{-2}(T, p)$ are observed at $T < T_c/2$ and $0.078 \leq p \leq 0.16$: (i) $n_s(0, p)$ depends linearly on p , (ii) the derivative $|dn_s(T, p)/dT|_{T \rightarrow 0}$ depends on p slightly in the optimally and moderately doped regions ($0.10 < p \leq 0.16$); however, it rapidly increases with p further lowering and (iii) the latter finding is accompanied by the linear low-temperature dependence $\Delta n_s(T) \propto (-T)$ changing to $\Delta n_s(T) \propto (-\sqrt{T})$. For optimum oxygen content the temperature dependence of the normalized imaginary part of the c -axis conductivity $\lambda_c^2(0)/\lambda_c^2(T)$ is found to be strikingly similar to that of $\lambda_{ab}^2(0)/\lambda_{ab}^2(T)$ and becomes more convex with p lowering. $\lambda_c^{-2}(0, p)$ values are roughly proportional to the normal state conductivities $\sigma_c(T_c, p)$ along the c -axis. All these properties can be treated in the framework of d -density wave order of pseudogap.

I. INTRODUCTION

Last years a lot of interest has been attracted by investigations of the nature of pseudogap states of high- T_c superconductors' (HTSC) phase diagram. This area corresponds to lower concentration p of holes per copper atom in the CuO_2 plane and lower critical temperatures T_c in comparison with the optimal value $p \approx 0.16$ and the maximum temperature $T_{c,max}$ of the superconducting transition. The p and T_c values in HTSC satisfy the following empirical relationship¹: $T_c = T_{c,max}[1 - 82.6(p - 0.16)^2]$. Currently, the origin of the pseudogap remains unclear. Proposed theoretical scenarios may be divided into two categories. One is based on the idea that the pseudogap is due to precursor superconductivity, in which pairing takes place at the pseudogap transition temperature $T^* > T_c$ but achieves coherence only at T_c . The other assumes that the pseudogap state is not related to superconductivity per se, but rather competes with it. This magnetic precursor scenario of the pseudogap assumes dynamical fluctuations of some kind, such as spin, charge or structural, or so-called staggered flux phase. These two scenarios treat anomalies of electronic properties in underdoped HTSC observed at temperatures both above T_c and in its vicinity^{2,3,4,5}.

In the heavily underdoped HTSC, at $T \ll T_c$ a competition of pseudogap and superconducting order parameters develops most effectively and results in the peculiarities of the superfluid density $n_s(T, p)$ as a function of T and p . It is well known that in clean BCS d -wave superconductors (DSC) the dependence $\Delta n_s(T) \equiv n_s(T) - n_0$ is linear on temperature $T \ll T_c$: $\Delta n_s(T) \propto (-T/\Delta_0)$, where $n_0 = n_s(0)$ and $\Delta_0 = \Delta(0)$ are the superfluid density and the superconducting gap amplitude at $T = 0$. This dependence is confirmed by the measurements of the ab -plane penetration depth $\lambda_{ab}(T) = \sqrt{m^*/\mu_0 e^2 n_s(T)}$: $\Delta \lambda_{ab}(T) \propto T$ at $T < T_c/3$, where μ_0 , m^* and e are the vacuum permeability, the effective mass and the electronic charge, respectively. The derivative $|dn_s(T)/dT|$ at $T \rightarrow 0$ determines n_0/Δ_0 ratio. If thermally ex-

cited fermionic quasiparticles are the only important excitations even at $p < 0.16$, then the slope of $n_s(T)$ curves at $T \ll T_c$ is proportional to $n_0(p)/\Delta_0(p)$ ratio: $|dn_s(T)/dT|_{T \rightarrow 0} \propto n_0(p)/\Delta_0(p)$. The measurements of $\lambda_{ab}(0)$ in underdoped HTSC showed that the superfluid density $n_0(p) \propto \lambda_{ab}^{-2}(0)$ increases approximately linearly with $p > 0.08$ reaching its maximum value at $p \approx 0.16$ ^{6,7}.

When decreasing $p < 0.16$ and hence approaching the dielectric phase, the role of electron correlations and phase fluctuations becomes increasingly significant. The generalized Fermi-liquid models (GFL) allow for this through p -dependent Landau parameter $L(p)$ ^{8,9,10} which includes $n_0(p)$. The values of $\Delta_0(p)$ and $L(p)$ determine the doping dependence of the derivative $|dn_s(T)/dT|_{T \rightarrow 0} = L(p)/\Delta_0(p)$. In Ref. 8 the ratio $L(p)/\Delta_0(p)$ does not depend on p ; the model⁹ predicts $L(p)/\Delta_0(p) \propto p^{-2}$. The measurements of $\text{YBa}_2\text{Cu}_3\text{O}_{7-x}$ single crystals¹¹ and oriented powders¹² with the holes concentration $p \gtrsim 0.1$ showed that the slope of $n_s(T)$ dependences at $T \rightarrow 0$ is either slightly p -dependent¹¹, which agrees with Ref. 8, or diminishes with decreasing $p \leq 0.16$,¹² which contradicts the GFL models^{8,9,10}.

In the precursor pairing model^{13,14} of pseudogap, based on the formation of pair electron excitations with finite momentum at $T^* > T_c$, the influence of pseudogap order parameter on the quasiparticles spectrum at $T < T_c$ leads to a rise of $\Delta_0(p)$ and decrease of $n_0(p)$ with p lowering. Hence, the decrease of the derivative $|dn_s(T)/dT|_{T \rightarrow 0} \propto n_0(p)/\Delta_0(p)$ is expected. The $n_s(T, p)/n_0$ dependences calculated in Ref. 14 show that their low temperature slopes decrease with underdoping. An alternative behavior of $|dn_s(T)/dT|$ follows from magnetic precursor d -density wave (DDW) scenario of pseudogap¹⁵. In this model a DDW order parameter $W(p, T)$ is directly introduced into the quasiparticle band structure. At low energies the excitation spectrum of DDW consists of conventional fermionic particles and holes like that of DSC with which it competes at $p < 0.2$. The DSC gap $\Delta_0(p)$ steadily vanishes with p decreasing, whereas the sum of zero-temperature squares $\Delta_0^2(p) + W_0^2(p)$ remains constant¹⁶. In the issue, the

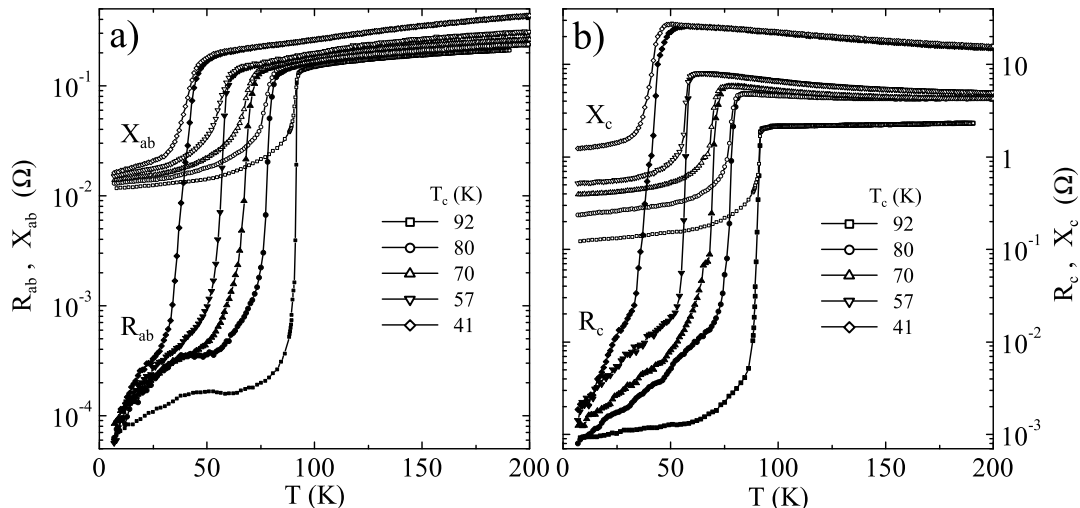


Figure 1: a) real $R_{ab}(T)$ (solid symbols) and imaginary $X_{ab}(T)$ (open symbols) parts of the ab -plane surface impedance of the five states of $\text{YBa}_2\text{Cu}_3\text{O}_{7-x}$ single crystal; b) the components of the c -axis surface impedance.

DDW model predicts a growth of the slope of $n_s(T, p)/n_0$ curves at low T and $p < 0.1$. At the same time the opening of pseudogap influences weakly the c -axis penetration depth $\lambda_c(T, p)$ of high-frequency field for currents running perpendicular to CuO_2 planes. In particular, strong decrease of the interlayer coupling integral $t_\perp(p)$ with p lowering¹⁷ in $\text{YBa}_2\text{Cu}_3\text{O}_{7-x}$ dominates over effects of the DDW order on $\lambda_c(0, p)$ ¹⁸.

The present paper aims at the experimental verification of the above mentioned theoretical speculations.

II. EXPERIMENT

To fulfill the task, we investigated the anisotropy and evolution of the temperature dependences of microwave conductivity components in $\text{YBa}_2\text{Cu}_3\text{O}_{7-x}$ crystal under varying oxygen doping in the range $0.07 \leq x \leq 0.47$. The crystal of a rectangular shape, with dimensions $1.6 \times 0.4 \times 0.1 \text{ mm}^3$, has been grown in a BaZrO_3 crucible. The measurements were made at the frequency of $\omega/2\pi = 9.4 \text{ GHz}$ and in the temperature range $5 \leq T \leq 200 \text{ K}$. To

change an oxygen content in the sample, we successively annealed the sample in the air at different $T \geq 500^\circ \text{ C}$ specified in Table 1.

According to susceptibility measurements at the frequency of 100 kHz, superconducting transition width amounted to 0.1 K in the optimally doped state ($x = 0.07$); however, the width increased with the increase of x , having reached 4 K at $x = 0.47$. The temperatures of the superconducting transition were $T_c = 92, 80, 70, 57, 41 \text{ K}$ which correspond to the concentrations $p = 0.16, 0.12, 0.106, 0.092, 0.078$, respectively (Table 1). Anisotropy was measured for each of the five crystal states. The whole cycle of the microwave measurements included the following: (i) we measured the temperature dependences of the quality factor and of the frequency shift of the superconducting niobium resonator with the sample inside in the two crystal orientations with respect to the microwave magnetic field, transversal (T) and longitudinal (L); (ii) measurements in the T orientation gave the surface resistance $R_{ab}(T)$, reactance $X_{ab}(T)$ and conductivity $\sigma_{ab}(T) = i\omega\mu_0/Z_{ab}^2(T)$ of the crystal cuprate planes in its normal and superconducting states; (iii) measurements in the L orientation gave $\sigma_c(T)$, $X_c(T)$, $R_c(T)$. See Ref. 19 for the details of the measuring technique in the optimally doped $\text{YBa}_2\text{Cu}_3\text{O}_{6.95}$ crystal.

Table I: Annealing and critical temperatures, doping parameters and penetration depths of $\text{YBa}_2\text{Cu}_3\text{O}_{7-x}$ crystal.

annealing $T, ^\circ\text{C}$	critical T_c, K	doping parameters		λ values at $T = 0$		$\Delta\lambda_c(T)$ $\propto T^\alpha$ α
		p	x	λ_{ab}, nm	$\lambda_c, \mu\text{m}$	
500	92	0.16	0.07	152	1.55	1.0
520	80	0.12	0.26	170	3.0	1.1
550	70	0.106	0.33	178	5.2	1.2
600	57	0.092	0.40	190	6.9	1.3
720	41	0.078	0.47	198	16.3	1.8

The temperature dependences of surface impedance $Z_{ab} = R_{ab} + iX_{ab}$ components, $R_{ab}(T)$ and $X_{ab}(T)$, are shown in Fig. 1a. In the normal state for each of the five crystal states we have $R_{ab}(T) = X_{ab}(T)$ which implies the validity of the normal skin-effect condition. The value of residual losses $R_{ab}(T \rightarrow 0)$ does not exceed $40 \mu\Omega$. In the case of optimum oxygen content $R_{ab}(T)$ dependence has a broad peak at $T \sim T_c/2$ which vanishes with p lowering. At $T < T_c/3$ all $R_{ab}(T)$ curves

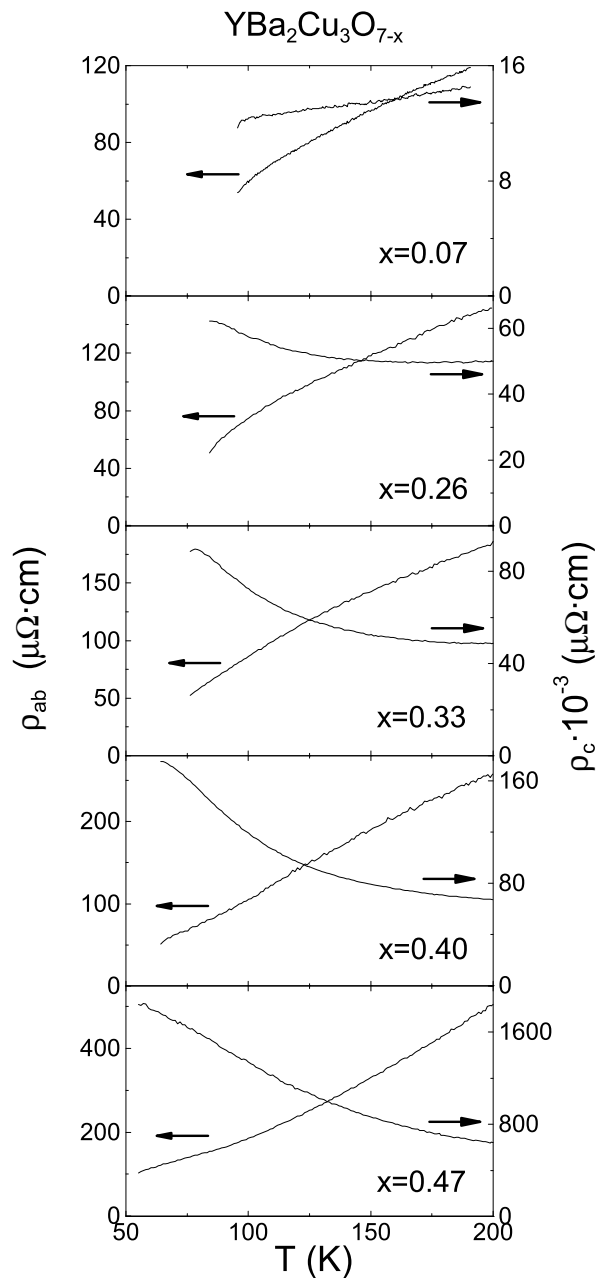


Figure 2: The evolution of the measured $\rho_{ab}(T)$ and $\rho_c(T)$ dependences in $\text{YBa}_2\text{Cu}_3\text{O}_{7-x}$ with different oxygen content.

are linear on T . In Fig. 1b we demonstrate the temperature dependences of the c -axis impedance components $R_c(T)$ and $X_c(T)$. The real and imaginary parts of the surface impedance coincide at $T > T_c$, $R_c(T) = X_c(T)$. Therefore, the resistivities $\rho_{ab}(T)$ and $\rho_c(T)$ can be found from $R_{ab}(T)$ and $R_c(T)$ curves at $T > T_c$ in Fig. 1, applying the standard formulas of the normal skin effect: $\rho_{ab}(T) = 2R_{ab}^2(T)/\omega\mu_0$, $\rho_c(T) = 2R_c^2(T)/\omega\mu_0$. Fig. 2 shows the evolution of the dependences $\rho_{ab}(T)$ and $\rho_c(T)$ in $\text{YBa}_2\text{Cu}_3\text{O}_{7-x}$ crystal with the change of x in the temperature range $T_c < T \leq 200$ K.

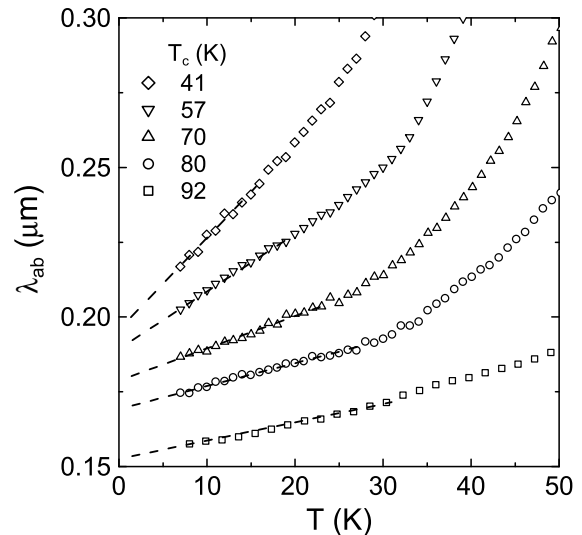


Figure 3: Low-temperature dependences of $\lambda_{ab}(T)$ (open symbols) measured for five states of $\text{YBa}_2\text{Cu}_3\text{O}_{7-x}$ crystal with $T_c = 92$ K, $T_c = 80$ K, $T_c = 70$ K, $T_c = 57$ K, and $T_c = 41$ K. Dashed lines are linear extrapolations at $T < T_c/3$.

III. RESULTS AND DISCUSSION

Fig. 3 shows the low temperature sections of the measured $\lambda_{ab}(T) = X_{ab}(T)/\omega\mu_0$ curves. The linear extrapolation (dashed lines) of these dependences at $T < T_c/3$ gives the following $\lambda_{ab}(0)$ values: 152, 170, 178, 190, 198 nm for $p = 0.16, 0.12, 0.106, 0.092, 0.078$, respectively (Table 1). The error in $\lambda_{ab}(T)$ is largely determined by the measurement accuracy of the additive constant X_0 which is equal to the difference between the measured reactance shift $\Delta X_{ab}(T)$ and $R_{ab}(T)$ at $T > T_c$ ²⁰.

As follows from Fig. 4, halving of the concentration (namely, from $p = 0.16$ to $p = 0.078$) results in approximately two times smaller $\lambda_{ab}^{-2}(0) = n_0\mu_0e^2/m^*$ value. Similar behavior $n_0(p) \propto p$ within the range $0.08 < p \leq 0.16$ was observed by other groups^{6,7}. It is easily seen that this dependence contradicts Uemura's relation $n_0(p) \propto T_c(p)$ ²¹. The naive linear extrapolation of the dashed line in Fig. 4 at $p < 0.08$ leads to nonphysical result: $n_0(p)$ is finite at vanishing p . To the best of our knowledge there is no data of superfluid density measurements in HTSC at $p < 0.08$. As for theoretical predictions, n_0 linearity on p extends down to $p = 0$ in the model⁸, while in the DDW scenario^{16,22} it exists in the underdoped range of phase diagram (Fig. 5) where the DSC order parameter grows from zero to its maximal value, moreover, $n_0(p)$ is nonzero as $\Delta_0(p)$ vanishes (Fig. 1 from Ref.²²). The latter agrees with our data.

In Fig. 4 we also show the slopes $|d\lambda_{ab}^{-2}(T)/dT|_{T \rightarrow 0} \propto |dn_s(T)/dT|_{T \rightarrow 0}$ of $\lambda_{ab}^{-2}(T)$ curves obtained from $\lambda_{ab}(T)$ dependences at $T < T_c/3$. The value of $|d\lambda_{ab}^{-2}(T)/dT|$ changes slightly at $0.1 < p \leq 0.16$ in accordance with Ref.⁸. However, it grows drastically at $p \lesssim 0.1$, namely,

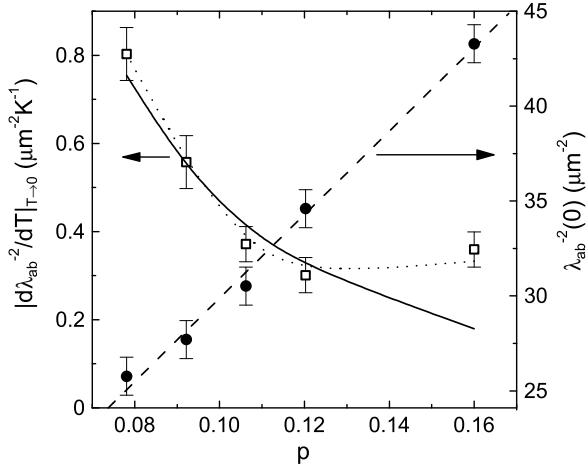


Figure 4: The values of $\lambda_{ab}^{-2}(0) = n_s(0)\mu_0e^2/m^*$ (right scale) and slopes $|d\lambda_{ab}^{-2}(T)/dT|_{T\rightarrow 0} = \mu_0e^2/m^*|dn_s(T)/dT|_{T\rightarrow 0}$ (left scale) as a function of doping $p = 0.16 - \sqrt{(1 - T_c/T_{c,max})/82.6}$ with $T_{c,max} = 92$ K in $\text{YBa}_2\text{Cu}_3\text{O}_{7-x}$. Error bars correspond to experimental accuracy. The dashed and dotted lines guide the eye. The solid line is $|dn_s(T)/dT| \propto p^{-2}$ dependence.

$\lambda_{ab}^{-2}(T)$ slope increases 2.5 times with p decrease from 0.12 to 0.08. $|d\lambda_{ab}^{-2}(T)/dT| \propto p^{-2}$ dependence⁹ is shown by solid line in Fig. 4 and roughly fits the data at $p \leq 0.12$. The dotted line drawn through $|d\lambda_{ab}^{-2}(T)/dT|$ experimental points in Fig. 4 qualitatively agrees with the behavior of this quantity in the DDW model^{16,22}.

The temperature dependence of the superfluid density

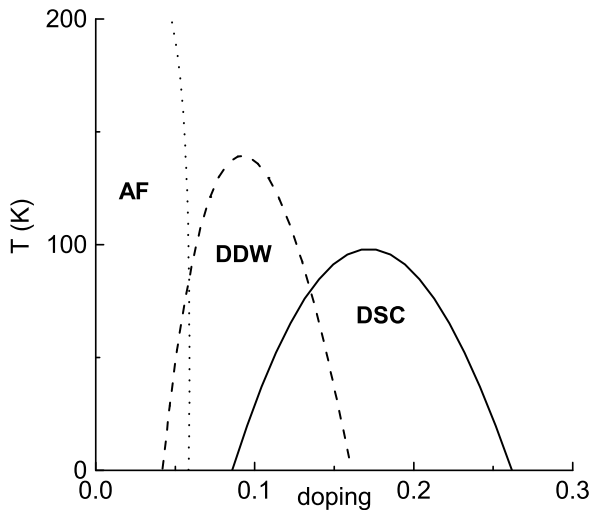


Figure 5: The temperature versus doping p schematic phase diagram based on calculations of Ref.²³. AF is the three-dimensional antiferromagnetic phase. The system is an insulator in the AF state, a metal in the DDW and DDW+AF states, and a superconductor in the DSC and DDW+DSC states²³.

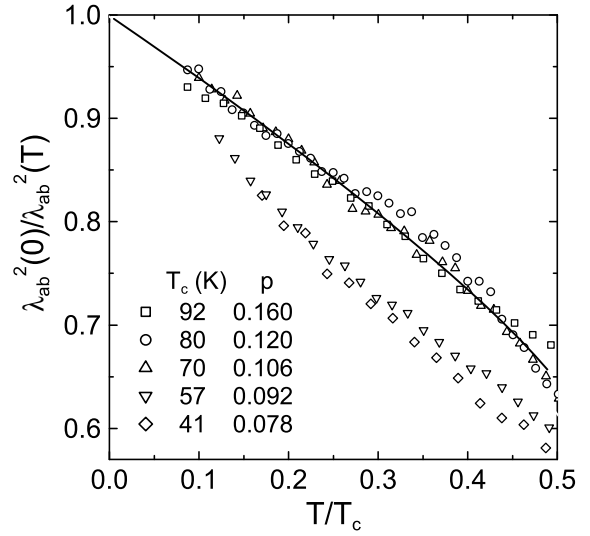


Figure 6: The measured dependences of $\lambda_{ab}^2(0)/\lambda_{ab}^2(T) = n_s(T)/n_s(0)$ at $T < T_c/2$ in $\text{YBa}_2\text{Cu}_3\text{O}_{7-x}$ with different doping. The solid line is the $\lambda_{ab}^2(0)/\lambda_{ab}^2(T)$ dependence in BCS d -wave superconductor (DSC).

$n_s(T)$ at low T in the heavily underdoped $\text{YBa}_2\text{Cu}_3\text{O}_{7-x}$ proves to be one more check-up of the DDW scenario of pseudogap. $\lambda_{ab}^2(0)/\lambda_{ab}^2(T) = n_s(T)/n_0$ dependences obtained from the data in Fig. 3 are shown in Fig. 6 for different p values. The solid line represents the DSC result. The evident peculiarities in Fig. 6 are the concavity of $n_s(T)/n_0$ curves corresponding to the heavily underdoped states ($p = 0.078$ and $p = 0.092$) and their deviation from DSC and the curves for $p = 0.16, 0.12, 0.106$. This behavior of the superfluid density $n_s(T)/n_0$ contradicts the conclusions of the precursor pairing model¹⁴, but agrees with the DDW scenario¹⁶. According to¹⁶, at temperatures much smaller than the relevant energy scales W_0 and Δ_0 , only the nodal regions close to the points $(\pi/2, \pi/2)$ and symmetry-related points on the Fermi surface will contribute to the suppression of the superfluid density. In a wide range of temperatures $n_s(T)$ dependence will be linear for the optimally and moderately doped samples, in which Δ_0 is larger than or comparable to W_0 (Fig. 5) and plays a leading role in the temperature dependence of the superfluid density. However, for the heavily underdoped samples the situation is quite different. As the DDW gap is much larger than the superconducting gap in these heavily underdoped samples, W_0 becomes dominant around the nodes. Though in the asymptotically low-temperature regime the suppression of the superfluid density is linear on temperature, there is an intermediate temperature range over which the suppression actually behaves as \sqrt{T} . It is worth emphasizing that the authors of Ref.¹⁶ state that these features are independent of the precise $W_0(p)$ and $\Delta_0(p)$ functional forms. The only input that is needed is the existence of DDW order which diminishes with

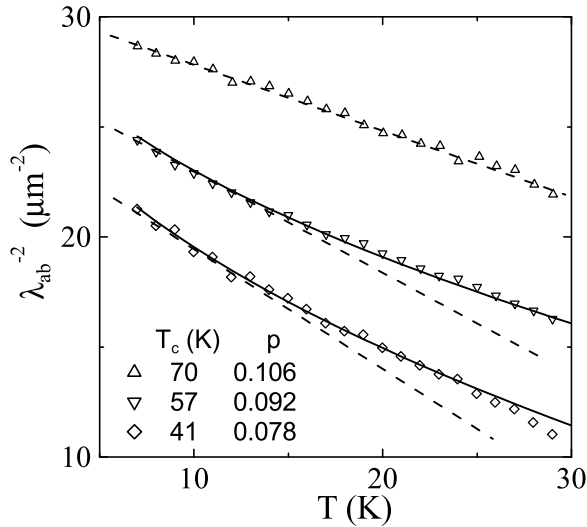


Figure 7: Comparison of experimental $\lambda_{ab}^{-2}(T) \propto n_s(T)$ curves (symbols) with linear $\Delta\lambda_{ab}^{-2}(T) \propto (-T)$ (dashed lines) and root $\Delta\lambda_{ab}^{-2}(T) \propto (-\sqrt{T})$ (solid lines) dependences for moderately doped ($p = 0.106$, $x = 0.33$) and heavily underdoped ($p = 0.092$, $x = 0.40$; $p = 0.078$, $x = 0.47$) $\text{YBa}_2\text{Cu}_3\text{O}_{7-x}$.

p increase and complementary development of the DSC order. The DDW order eats away part of the superfluid density from an otherwise pure DSC system. Actually, in the intermediate temperature range $0.1T_c < T \lesssim 0.5T_c$ the experimental $n_s(T)$ curves in $\text{YBa}_2\text{Cu}_3\text{O}_{6.60}$ and $\text{YBa}_2\text{Cu}_3\text{O}_{6.53}$ with $p < 0.1$ are not linear but similar to \sqrt{T} -dependences. This is confirmed by Fig. 7, where the measured curves $\lambda_{ab}^{-2}(T) \propto n_s(T)$ are compared with linear ($\propto T$) in $\text{YBa}_2\text{Cu}_3\text{O}_{6.67}$ ($p = 0.106$) and \sqrt{T} -dependences $\Delta\lambda_{ab}^{-2}(T) = -3\sqrt{T}$ (λ_{ab} and T are expressed in μm and K) in $\text{YBa}_2\text{Cu}_3\text{O}_{6.60}$ ($p = 0.092$) and $\Delta\lambda_{ab}^{-2}(T) = -3.5\sqrt{T}$ in $\text{YBa}_2\text{Cu}_3\text{O}_{6.53}$ ($p = 0.078$). Dashed lines in Fig. 7 correspond to the linear at $T < T_c/3$ dependences of $\lambda_{ab}(T)$ presented in Fig. 3 and extended to higher temperatures.

It is also interesting to note that these deviations of $\Delta\lambda_{ab}^{-2}(T)$ in $\text{YBa}_2\text{Cu}_3\text{O}_{6.60}$ and $\text{YBa}_2\text{Cu}_3\text{O}_{6.53}$ are accompanied by inflection of the resistivity $\rho_{ab}(T)$ curves in the normal state of these samples. These inflections are seen at two lower $\rho_{ab}(T)$ curves in Fig. 2 around $T \sim 100$ K. One more feature of the curves in Fig. 2 is that only the optimally doped $\text{YBa}_2\text{Cu}_3\text{O}_{6.93}$ shows that both dependences $\rho_{ab}(T)$ and $\rho_c(T)$ have a metallic behavior, and the ratio ρ_c/ρ_{ab} approaches the anisotropy of effective masses of charge carriers $m_c/m_{ab} = \lambda_c^2(0)/\lambda_{ab}^2(0)$ in 3D London superconductor, which type $\text{YBa}_2\text{Cu}_3\text{O}_{6.93}$ belongs to. The other states of $\text{YBa}_2\text{Cu}_3\text{O}_{7-x}$ have the resistivity $\rho_c(T)$ increase with the decrease of temperature, so that decrease of carriers concentration in $\text{YBa}_2\text{Cu}_3\text{O}_{7-x}$ crystal results in the crossover from Drude c -axis conductivity to the tunneling one²⁴. The evolution of the temperature de-

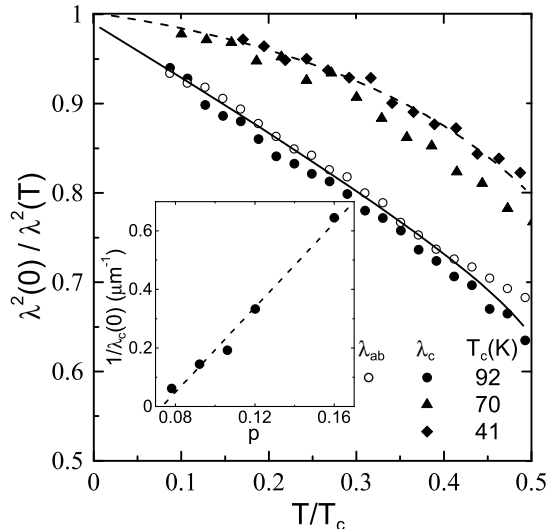


Figure 8: The dependence $\lambda_{ab}^2(0)/\lambda_{ab}^2(T)$ (open symbols) in $\text{YBa}_2\text{Cu}_3\text{O}_{6.93}$ and $\lambda_c^2(0)/\lambda_c^2(T)$ (full symbols) measured for three states of the $\text{YBa}_2\text{Cu}_3\text{O}_{7-x}$ crystal with $T_c = 92$ K, $T_c = 70$ K and $T_c = 41$ K. Solid and dashed lines stand for the dependences $\lambda_c^2(0)/\lambda_c^2(T)$ calculated in Ref. 25 for $\text{YBa}_2\text{Cu}_3\text{O}_{7-x}$ with different oxygen deficiency. The inset shows $1/\lambda_c$ at $T = 0$ as a function of doping p .

pendences of $\rho_c(T)$ with doping correlates with those of the c -axis penetration depth $\lambda_c(T)$. Solid symbols of Fig. 8 show the dependences $\lambda_c^2(0)/\lambda_c^2(T)$ at $T \leq T_c/2$ for $\text{YBa}_2\text{Cu}_3\text{O}_{7-x}$ states with $T_c = 92$ K, $T_c = 70$ K and $T_c = 41$ K. Table 1 contains the values of the penetration depth $\lambda_c(0)$ at $T = 0$ and the exponents α in the measured $\lambda_c(T) - \lambda_c(0) = \Delta\lambda_c(T) \propto T^\alpha$ dependences at $T \leq T_c/3$. The peculiarity of the optimally doped state $\text{YBa}_2\text{Cu}_3\text{O}_{6.93}$ is good coincidence of $\lambda_{ab}^2(0)/\lambda_{ab}^2(T)$ (open circles in Fig. 8) and $\lambda_c^2(0)/\lambda_c^2(T)$ temperature dependences. With the decrease of p the temperature dependence of $\lambda_c^2(0)/\lambda_c^2(T)$ becomes substantially weaker than that of $\lambda_{ab}^2(0)/\lambda_{ab}^2(T)$. Model²⁵ associates the reduction in the low- T slope of $\lambda_c^2(0)/\lambda_c^2(T)$ curves and the appearance of semiconducting-like temperature dependence of $\rho_c(T)$ with a decrease of the interlayer coupling in the crystal. Dashed line in Fig. 8 represents numerical result²⁵ for this case. On the other hand, in the optimally doped $\text{YBa}_2\text{Cu}_3\text{O}_{6.93}$ the interlayer coupling is strong and quasiparticle transport along the c -axis becomes identical to one in the anisotropic 3D superconductor²⁶. Solid line in Fig. 8 is $\lambda_c^2(0)/\lambda_c^2(T)$ dependence, calculated in Ref. 25 for this particular case. So, the low- T dependences of $\lambda_c(T)$ are well described without taking pseudogap effects into consideration. Let us consider now their possible manifestations in the doping dependence of the c -axis penetration depth.

From the inset to Fig. 8 follows that reciprocal value of the zero-temperature penetration depth $1/\lambda_c(0, p)$ is roughly linear on p . Note that it vanishes at $p \approx 0.07$

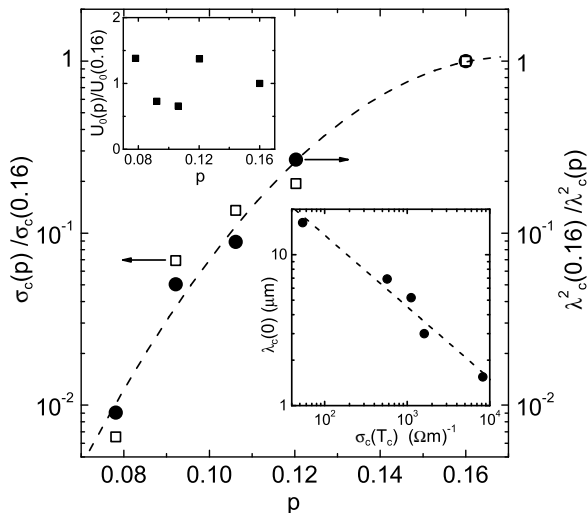


Figure 9: Doping dependences of $\lambda_c^2(p)/\lambda_c^2(0.16)$ at $T = 0$ and $\sigma_c(p)/\sigma_c(0.16)$ at $T = T_c$. Their ratio $U_0(p)/U_0(0.16)$ is shown in the upper inset. The lower inset is $\lambda_c(0)$ versus $\sigma_c(T_c)$ plot.

which is near the value where T_c does too (Fig. 5). There are several theoretical models^{25,27} and experimental confirmations²⁸ of the direct proportionality of $\lambda_c^{-2}(0)$ to the c -axis conductivity $\sigma_c(T_c)$ in HTSC. In the simplest theory this correlation is caused by $\lambda_c^{-2} \propto J_c$ relation, where J_c is the c -axis critical current in the d -wave superconductor with anisotropic interlayer scattering and weak interlayer coupling. The value of $J_c(0)$ is determined by both the superconducting gap Δ_0 and the conductivity $\sigma_c(T_c)$. The symbols in the lower inset to Fig. 9 show our data fitted by the dashed line

$\log \lambda_c(0)[\mu\text{m}] = -0.48 \log \sigma_c(T_c)[\Omega^{-1}\text{m}^{-1}] + 2.08$. The latter constant defines a proportionality factor $U_0(p)$ in $\lambda_c^{-2}(0, p) = U_0(p) \sigma_c(T_c, p)$ relation. In the framework of DDW model the value of $U_0(p)$ is determined by the doping dependences of $\Delta_0(p)$, $W_0(p)$ and chemical potential $\mu(p)$. As it is shown in Ref.¹⁸ the opening of DDW gap can lead to increase as well as to decrease of $U_0(p)$. This depends on the position of Fermi surface with respect to DDW gap, but in any case $U_0(p)$ changes less than twice in the whole range of doping. The values of $\lambda_c^2(0.16)/\lambda_c^2(p)$ at $T = 0$ and $\sigma_c(p)/\sigma_c(0.16)$ at $T = T_c$ are shown in Fig. 9. Their ratio $U_0(p)/U_0(0.16)$ is demonstrated in the upper inset to Fig. 9. This weak doping dependence indicates that the contribution of the interlayer coupling integral $t_{\perp}(p) \propto \sigma_c(T_c, p)$ into $\lambda_c(0, p)$ is dominant.

Thus, four main experimental observations of this paper, viz, (i) linear dependence of $n_0(p)$ in the range $0.078 \leq p \leq 0.16$, (ii) drastic increase of low-temperature $n_s(T)$ slope at $p < 0.1$, (iii) the deviation of $\Delta n_s(T)$ dependence from universal BCS behavior $\Delta n_s(T) \propto (-T)$ at $T < T_c/2$ towards $\Delta n_s(T) \propto (-\sqrt{T})$ with decreasing $p < 0.1$, and (iv) very weak influence of pseudogap on the low- T and doping dependences of the c -axis penetration depth evidence the DDW scenario of electronic processes in underdoped HTSC. Nevertheless, the measurements of $\lambda_{ab}(T)$ and $\lambda_c(T)$ at lower temperatures and in the high-quality samples with smaller carrier density are necessary for ultimate conclusion.

Helpful discussions with A.I. Larkin, E.G. Maksimov, and Sudip Chakravarty are gratefully acknowledged. This research was supported by RFBR grants Nos. 03-02-16812 and 02-02-08004.

-
- ¹ J.L. Tallon, C. Bernhard, H. Shaked et al., Phys. Rev. B **51**, 12911 (1995).
 - ² T. Timusk and B. Statt, Rep. Prog. Phys. **62**, 61 (1999).
 - ³ J.L. Tallon and J.W. Loram, Physica C **349**, 53 (2001).
 - ⁴ M.V. Sadovskii, Usp. Fiz. Nauk **171**, 539 (2001) [Phys. Usp. **44**, 515 (2001)].
 - ⁵ M.R. Norman and C. Pépin, cond-mat/0302347.
 - ⁶ J.W. Loram, J. Luo, J.R. Cooper et al., J. Phys. Chem. Solids **62**, 59 (2001).
 - ⁷ C. Bernhard, J.L. Tallon, Th. Blasius et al., Phys. Rev. Lett. **86**, 1614 (2001).
 - ⁸ P.A. Lee and X-G. Wen, Phys. Rev. Lett. **78**, 4111 (1997).
 - ⁹ A.J. Millis, S.M. Girvin, L.B. Ioffe, A.I. Larkin, J. Phys. Chem. Solids **59**, 1742 (1998).
 - ¹⁰ L.B. Ioffe and A.J. Millis, J. Phys. Chem. Solids **63**, 2259 (2002).
 - ¹¹ D.A. Bonn, S. Kamal, A. Bonakdarpour et al., Czech. J. Phys. **46**, 3195 (1996).
 - ¹² C. Panagopoulos, J.R. Cooper, and T. Xiang, Phys. Rev. B **57**, 13422 (1998).
 - ¹³ I. Kostzin, Q. Chen, Y-J. Kao et al., Phys. Rev. B **61**, 11662 (2001).
 - ¹⁴ K. Levin, Q. Chen, I. Kostzin et al., J. Phys. Chem. Solids **63**, 2233 (2002).
 - ¹⁵ S. Chakravarty, R.B. Laughlin, D.K. Morr et al., Phys. Rev. B **63**, 094503 (2001).
 - ¹⁶ S. Tewari, H-Y. Kee, C. Nayak et al., Phys. Rev. B **64**, 224516 (2001).
 - ¹⁷ P. Nyhus, M.A. Karlow, S.L. Cooper et al., Phys. Rev. B **50**, 13898 (1994).
 - ¹⁸ W. Kim, J.-X. Zhu, J.P. Carbotte et al., Phys. Rev. B **65**, 064502 (2002).
 - ¹⁹ Yu.A. Nefyodov, M.R. Trunin, A.A. Zhohov et al., Phys. Rev. B **67**, 144504 (2003).
 - ²⁰ M.R. Trunin, Yu.A. Nefyodov, and A.F. Shevchun, Phys. Rev. Lett. (2004, in press); see also cond-mat/0312566.
 - ²¹ Y.J. Uemura, Physica C **282-287**, 194 (1997).
 - ²² Q.-H. Wang, J.H. Han, and D.-H. Lee, Phys. Rev. Lett. **87**, 077004 (2001).
 - ²³ C. Nayak and E. Pivovarov, Phys. Rev. B **66**, 064508 (2002).
 - ²⁴ M.R. Trunin and Yu.A. Nefyodov, Pis'ma v ZhETF

- 77**(10), 696 (2003) [JETP Lett. **77**(10), 592 (2003)], cond-mat/0306158.
- ²⁵ R.J. Radtke, V.N. Kostur, and K. Levin, Phys. Rev. B **53**, R522 (1996).
- ²⁶ T. Xiang, C. Panagapoulos, and J.R. Cooper, Int. Journ. Mod. Phys. B **12**, 1007 (1998).
- ²⁷ P.J. Hirschfeld, S.M. Quinlan, and D.J. Scalapino, Phys. Rev. B **55**, 12742 (1997); S. Chakravarty, H.-Y. Kee, and E. Abrahams, Phys. Rev. Lett. **82**, 2366 (1999); Y. Ohashi, J. Phys. Soc. Jpn. **69**, 659 (2000).
- ²⁸ D.N. Basov, T. Timusk, B. Dabrowski et al., Phys. Rev. B **50**, 3511 (1994); J.R. Kirtley, K.A. Moler, G. Villard et al., Phys. Rev. Lett. **81**, 2149 (1998); S.V. Dordevic, E.J. Singley, D.N. Basov et al., Phys. Rev. B **65**, 134511 (2002).